Magnetization and susceptibility of ion-irradiated granular magnetite films

W. Jiang,* J. S. McCloy, and A. S. Lea
Pacific Northwest National Laboratory, Richland, Washington 99352, USA

J. A. Sundararajan, Q. Yao, and Y. Qiang
Physics Department, University of Idaho, Moscow, Idaho 83844, USA
(Received 11 November 2010; published 26 April 2011)

Porous granular films of magnetite (Fe_3O_4) with grains of ~3 nm in size were prepared using a state-of-the-art nanocluster deposition system. The films are initially superparamagnetic but become magnetized following Si^{2+} ion irradiation. A significant increase in the grain size and a dramatic change in the microstructure are observed. There are dipolar interactions between the nanoparticles in both the unirradiated and irradiated films. The in-phase alternating current magnetic susceptibility of the unirradiated film shows a blocking temperature of ~150 K, depending on frequency. A broadened Verwey transition for the irradiated film occurs at ~75 K, above which the susceptibility exhibits unusual behavior: a nearly linear decrease with decreasing temperature. There are irreversible domain rotations in the irradiated film during zero-field cooling and warming cycles between 10 and 300 K. The observed behavior of the irradiated granular films is quite distinct from that of metallic nanostructures after irradiation, and is due to the dramatic change in microstructures.

DOI: 10.1103/PhysRevB.83.134435 PACS number(s): 75.75.−c, 75.30.Kz, 61.80.Jh

I. INTRODUCTION

Magnetic nanostructured materials, including thin films and multilayer structures, have attracted considerable attention in recent years because of new science[1] and interesting properties.[2,3] The studies are driven primarily by advances in the synthesis of complex structures and motivated by the demands for higher-density information recording media. Magnetic ordering induced by 2.25 MeV proton irradiation in graphite was observed and attributed to spontaneous magnetization from hydrogenated carbon atoms.[4] Extensive irradiation studies have been performed on metallic structures, including Co/Pt multilayers[5–7] and thin films of Co/Fe (Ref. 8), Co/Cu (Ref. 9), FePt (Ref. 10), and NiFe (Ref. 11). The modified magnetic properties due to ion irradiation include a reduction in coercivity and remanent magnetization, a loss of magnetic anisotropy, and a transition of the easy axis. Various mechanisms responsible for the changes have been proposed, such as defect production, lattice strain release, interface roughening, and atomic mixing at the interfaces. Those studies have contributed to the understanding of the property changes induced by microstructural modifications.

In contrast, very few irradiation studies have been conducted to date on porous granular films, in part because of the limited availability of the films. Recently, we have found that the magnetic properties of $FeO + Fe_3N$ granular films, including remanence, saturation magnetization, and coercivity, are very resistant to room-temperature He^+ ion irradiation up to a fluence of 3×10^{15} ions/cm^2.[12] While this robustness is attractive for a variety of applications, including high-density recording media, more research is still needed to develop a fundamental understanding of the irradiation hardness and its dependence on dose, temperature, etc. Generally, magnetic properties of porous granular films are expected to be susceptible to ionizing radiation because of their large surface area. A slight change in bond distances and angles or the atomic coordination number at surfaces and interfaces of nanostructures can dramatically affect the magnetic behavior.[13] Understanding irradiation-induced modification of the magnetic properties of granular films is critical for controlling the properties and designing advanced devices with irradiation-resistant or -sensitive materials. This study reports on the response of granular magnetite (Fe_3O_4) films to ion irradiation near room temperature. Magnetite is selected as a model composition in this study. The results from this study show that the granular magnetite films are susceptible to ion irradiation, but their irradiation response is quite different from metallic nanostructures. The films represent a new class of semidisordered magnetite materials for study, which could lead to important applications of this type of material in various areas, including radiation detection and monitoring.

II. EXPERIMENTAL PROCEDURES

Granular films of cubic phase Fe_3O_4 nanoparticles used in this study were prepared using a state-of-the-art nanocluster deposition system.[14] The nanoparticles were formed in the aggregation chamber, where sputtered Fe atoms were fully oxidized and aggregated through low-temperature condensation. A high-transmission mass selector integral to the system was used to achieve a narrow particle size distribution (~5%). The selected nanoparticles landed softly onto a Si (100) substrate at room temperature in the deposition chamber. For the film used in this study, a total of 0.344 mg Fe_3O_4 nanoparticles were uniformly deposited over an area of 4×8 mm^2, corresponding to an areal density of 1.075×10^{-3} g/cm^2 or a film thickness of ~2.07 μm based on the theoretical specific gravity of 5.197 g/cm^3 for Fe_3O_4. The actual linear thickness is larger because of the film porosity. The magnetic properties of the film (for Figs. 1 and 2) after irradiation are compared to those of the same film before irradiation or a film (0.184 mg Fe_3O_4) prepared under the same conditions (for Figs. 3–5).

Ion irradiation was performed using a 3.0 MV electrostatic tandem accelerator (NEC 9SDH-2 pelletron, Middleton, WI). The granular film was irradiated at normal incidence with

5.5 MeV Si^{2+} ions to a fluence of 10^{16} ions/cm^2 near room temperature. A beam rastering system was used to ensure uniform irradiation over an area of 12.5 × 12.5 mm^2 covering the entire sample surface. Typical ion flux was on the order of 0.01 (Si^{2+}/nm^2)/s and the increase of the sample temperature was less than 50 K during the irradiation. Computer simulations with the Stopping and Range of Ions in Matter (SRIM) code[15] were carried out to estimate the ion projected range in the film. Based on the theoretical specific gravity of Fe_3O_4, the ion projected range under the irradiation condition is ∼2.1 μm with a full width at half maximum (FWHM) of ∼0.3 μm. Thus, the implanted Si is peaked near the film-substrate interface in this study.

The magnetic properties were measured for the as-deposited and post-irradiated films using a Physical Property Measurement System (PPMS, Quantum Design, San Diego, CA). After irradiation, the sample was placed in zero fields for remanence measurement at room temperature. Subsequent hysteresis measurement with the external field applied parallel to the sample surface was performed starting from 10 kOe. In-phase and out-of-phase alternating current (ac) magnetic susceptibilities (χ' and χ'', respectively) were also measured at frequencies of 0.03, 0.1, 1, and 10 kHz with an applied ac field of 5 Oe during zero-field cooling from 300 to 10 K at 10 K intervals, after waiting for 1 min at each temperature for stabilization. Saturated isothermal remanent magnetization (SIRM) for the irradiated sample was obtained by setting a direct current (dc) field of 2.5 T for 1 min at 300 K. After removing the field, the magnetization of the film was measured during cooling to 10 K and rewarming to 300 K. The crystal structure of the film was analyzed using the Philips X'pert Multi-Purpose Diffractometer (MPD, PANalytical, Almelo, The Netherlands) based on fixed Cu $K\alpha$ radiation ($\lambda = 0.154\,187$ nm). Grazing-angle incidence x-ray diffraction (GIXRD) was employed to study the crystallographic phase and average size of the crystalline grains at room temperature. This technique eliminates the strong diffraction peaks from the single-crystal substrate. The film microstructures were examined using a recently developed helium ion microscope (HIM, Orion Plus, Carl Zeiss SMT, Peabody, MA) before and after irradiation. In addition, magnetic force microscopy (MFM) was used to study the magnetic domains in the unirradiated and irradiated samples. MFM images were obtained using a multimode atomic force microscope (AFM, Digital Instruments, Nanoscope IIIA, Veeco Metrology, Santa Barbara, CA), a cobalt-coated probe tip (MESP, 70 kHz), and a lift height of ∼20 nm.

III. RESULTS AND DISCUSSION

A. Change in magnetic behavior

Figure 1 shows the hysteresis loops, taken at 300 K, for a granular Fe_3O_4 film before and after Si^{2+} ion irradiation, where the small diamagnetic and ferromagnetic signals from the Si substrate and sample holder have been subtracted. Before irradiation, the film does not possess any detectable magnetic remanence or coercivity at room temperature. The magnetization of the unirradiated film is not saturated at the maximum applied field of 10 kOe, where the corresponding value is

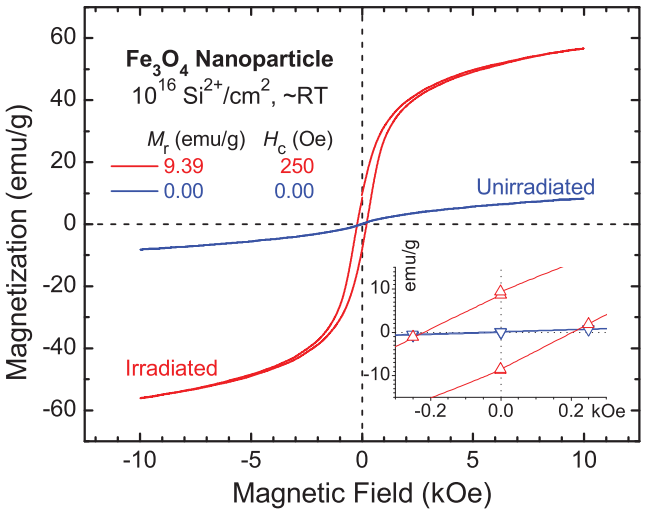

FIG. 1. (Color online) Hysteresis loops of a granular Fe_3O_4 film on Si before and after irradiation to a fluence of 10^{16} Si^{2+}/cm^2 near room temperature. The inset shows a magnified view near zero fields.

∼8.2 emu/g. After irradiation, the film becomes magnetized with a remanence of 9.4 emu/g at room temperature. This change of magnetic property is solely a result of the irradiation. By applying a magnetic field parallel to the sample surface, a hysteresis measurement was subsequently performed, and the data are shown in Fig. 1, where a completely different magnetization behavior is observed. The irradiated film shows a coercivity of 250 Oe and an unsaturated magnetization of 56 emu/g at 10 kOe. The remanent magnetization remained nearly unchanged before and after the hysteresis measurement.

B. Grain growth and particle aggregation

To understand the change in the magnetic properties of the irradiated granular Fe_3O_4 film, a number of characterizations have been performed to study the microstructures and magnetic domains. Figure 2 shows GIXRD patterns for the unirradiated and irradiated films, where the pattern intensity

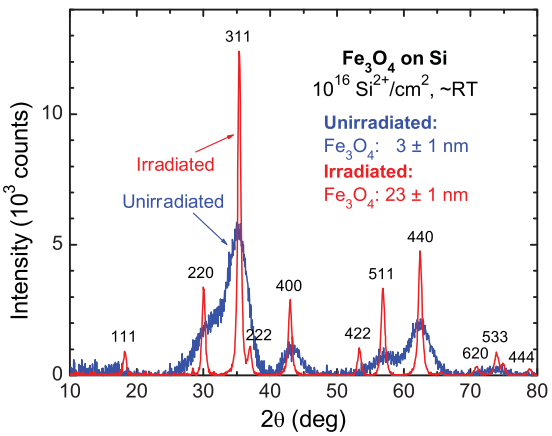

FIG. 2. (Color online) Backgroundsubtracted GIXRD patterns for a granular Fe_3O_4 film on Si before and after irradiation. The pattern intensity for the unirradiated film is multiplied by a factor of 4.

for the unirradiated sample was multiplied by a factor of 4 for a better comparison. The data indicate that the film is a single-phase cubic magnetite (Fe_3O_4) prior to irradiation. Neglecting small lattice strain, the average grain size, s, is estimated using the Scherrer equation,[16]

$$s = K \times \lambda/[\mathrm{FW}(S) \times \cos\theta], \quad (1)$$

where FW(S) is the specimen broadening (peak FWHM after subtraction of the instrument broadening), θ is the peak position, and K is the shape factor of the average crystallite, which is taken as 0.9 in the estimation. Using Eq. (1), the average grain size for the unirradiated film was determined to be 3 ± 1 nm based on the well-resolved (400) peak. Following irradiation, the diffraction peaks from all the observable planes become much stronger and sharper, but the crystalline phase (cubic Fe_3O_4) remains unchanged, as shown in Fig. 2. The average grain size for the irradiated film is estimated to be 23 ± 1 nm based on the (400) peak.

Depending on material composition, irradiation temperature, and dose rate, ion irradiation can induce amorphization or crystallization at the surface or interface of crystalline particles, resulting in grain shrinkage or growth. Previous studies have observed grain boundary amorphization[17,18] and crystallization[19,20] for different ceramic materials under ion irradiation. The observed significant increase in the Fe_3O_4 grain size in this study could be attributed to radiation-enhanced epitaxial growth and possibly coalescence of smaller crystalline grains.

High-resolution HIM for the films before and after irradiation was also performed to study the microstructural changes. This new technique shows advantages over the conventional scanning electron microscopy (SEM) in that it has a larger depth of field, a higher image contrast, a better spatial resolution, and a higher surface sensitivity. The high-resolution HIM micrographs for the film before and after irradiation are shown in Fig. 3. From Fig. 3(a), the unirradiated film exhibits nanoparticles loosely interconnected with each other in the film. The nanoparticles have a typical size of ~10 nm and each may contain several crystalline grains (~3 nm in size) with different orientations. The film is highly porous with large surface and interface areas. Irradiation leads to grain growth and particle aggregation. The resulting structure is complex with varied particle sizes. Clearly, the constituent nanoparticles are networked more tightly. Adhesion of the Fe_3O_4 film to the Si substrate is also found to be much stronger. As will be discussed below, the structural modification is mainly a result of electronic energy deposition of the 5.5 MeV Si^{2+} ions during irradiation. Nuclear energy deposition that generates atomic displacements becomes important only near the film-substrate interface just before the implanted Si ions reach their projected range.

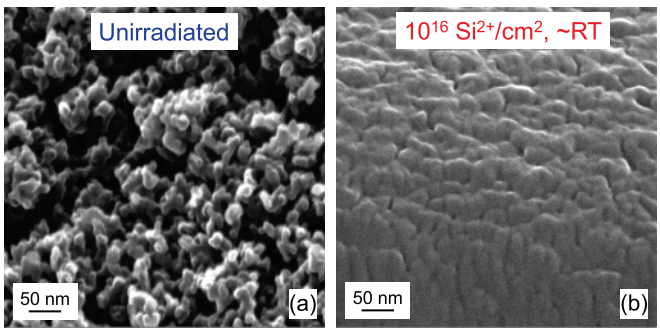

FIG. 3. (Color online) High-resolution HIM micrographs of granular Fe_3O_4 films on Si before and after irradiation.

A change in the grain or particle size and an alteration in the interatomic and electronic configurations at the grain or particle surfaces and interfaces can change magnetic properties. Before ion irradiation, crystalline grains in the film are small (~3 nm) and one particle (~10 nm in size) may contain several grains. Each grain has a single magnetic domain that is relatively free to rotate. Random orientation of the grain magnetic moments driven by thermal agitation at room temperature leads to a complete cancellation of magnetization or zero remanent magnetization. When an external field is applied, the magnetic moments of the individual grains and aggregated particles tend to align with the field by rotation to minimize the system energy. This leads to magnetic anisotropy and magnetization of the film. Once the external field is removed, thermal randomization of the moment orientation occurs, resulting in vanishing magnetization. The process is reversible and the unirradiated film does not show coercivity. This behavior is similar to that of paramagnetic materials, such as metals, that contain unpaired electrons. The unirradiated Fe_3O_4 film consisting of small domains with a larger moment is identified to be superparamagnetic. Since the nanoparticles are only loosely interconnected, the easy axes of magnetization for the unirradiated sample are expected to be randomly distributed.

Ion irradiation is a process of energy deposition into a material through both elastic and inelastic interactions between the energetic ions and electrons or nuclei in the material. As predicted by SRIM simulations,[15] elastic collisions that produce atomic displacements are important only near the film-substrate interface in this study. Inelastic interactions lead to electron excitation and ionization of the target atoms throughout the entire film thickness. A large amount of the primary ion energy is eventually coupled to phonons in the inelastic collision processes, which induce an increase in local temperature along the ion track. The inelastic process can enhance epitaxial crystallization at the amorphous-crystalline interface and promote coalescence of small crystalline grains, as observed from Fig. 3(b).

As grains grow and nanoparticles aggregate during ion irradiation, magnetic domains expand through ion-beam enhanced nucleation and growth, domain-wall motion, and domain rotation. Nucleation and growth of magnetic domains could take place at defects, such as grain boundaries. Domain rotation could be associated with the radiation-induced modification of the interatomic and electronic structures at the grain or particle surfaces, leading to a change in the bond distance or angles and the coordination number. The resulting larger grain (~23 nm in size) is expected to still have a single magnetic domain because the formation of a flux-closure configuration is energetically unfavorable at this small size of magnetite. The critical size for superparamagnetism in magnetite at room temperature is known to be 17–30 nm for low-frequency susceptibility measurements[21–23] but is smaller for shorter measurement times (9 nm for Mossbauer measurements).[24]

Domain-wall motion proceeds as grains grow and neighboring particles interact, leading to a much larger domain size than the particle dimension (see MFM data below). However, the distribution of the moment orientation is largely random at room temperature. A majority of the magnetic moments cancel themselves in the film, but a complete cancellation does not occur because of the structural inhomogeneity and imperfection with complex grain boundaries and different grain sizes that may create some high-energy barriers. These energy barriers must be overcome to rotate the local moment. At room temperature, thermal energy is not high enough to activate the rotation process. Thus, a small remanence in the film emerges. When an external field is applied, domains tend to align with the external field. In the magnetization process, domain-wall pinning is evident since the loop (Fig. 1) is not a perfect square. Domain rotation and possible nucleation and growth at structural defects are expected to be the primary mechanisms, although wall propagation cannot be completely ruled out. A nearly identical remanent magnetization remains once the external field is removed because the atomic structure of the film is largely unaffected during the magnetization and demagnetization processes. An opposite field must be applied ($H_c = 250$ Oe) to completely cancel the magnetization in the film. The observed behavior of the irradiated film is characteristic of ferromagnetism.

From the discussion above, it is apparent that the granular Fe_3O_4 film underwent a change from superparamagnetic to ferromagnetic behavior during the ion irradiation. It should be pointed out that there may also be a superparamagnetic component in the irradiated film due to the existence of smaller particles in the film. For multilayer structures, changes in magnetic properties due to ion irradiation are quite different. A previous study on thin Pt/Co/Pt/Al_2O_3 films[2] reported a reduction in the magnetocrystalline anisotropy, a spin orientation transition from easy axis out-of-plane to easy axis in-plane, and a change from ferromagnetic to paramagnetic behavior at progressively higher doses of He^+ ion irradiation. The physical interpretations were based on lattice relaxation, ion-beam-induced atomic mixing, and interface roughening. Similar effects of Ga^+ ion irradiation on a Co/Pt multilayer were also reported.[25]

C. Magnetic domains

To study the magnetic domains, examinations of the unirradiated and irradiated films were carried out using MFM. The AFM surface topography for the unirradiated and irradiated films is shown in Figs. 4(a) and 4(c), respectively. The magnetic force gradient was measured by monitoring the shift in resonant frequency of the oscillating tip due to the influence of the magnetic field. In this mode, the topography of the surface is initially obtained on a line-by-line basis using intermittent contact. After the topography of each line is obtained, the tip retraces the same topography in an interleaved fashion, but at a predefined distance (lift height) above the surface. At this height, the long-range magnetic force dominates any interaction between the tip and sample. For this particular study, the resonant vibration frequency of the cantilever was 61.7 kHz, the respective lift heights for the unirradiated and irradiated samples were 20.5 and 20.3 nm,

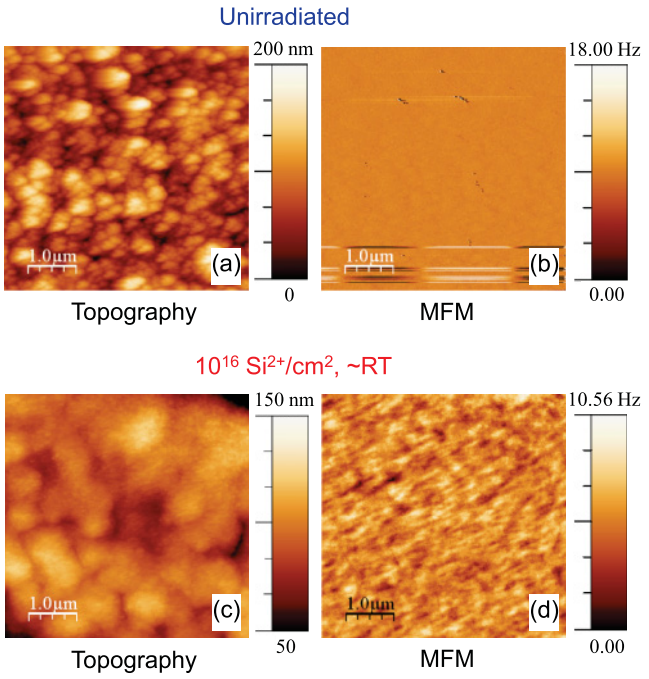

FIG. 4. (Color online) AFM and MFM images for granular Fe_3O_4 films on Si before and after irradiation.

and the detection limit for the frequency shift was ~0.1 Hz. The spatial resolution for the magnetic field imaging was on the order of 50 nm due to the $1/r^2$ dependence of the magnetic force. The MFM images shown in Figs. 4(b) and 4(d) for the unirradiated and irradiated films, respectively, are the result of the measured frequency shift in the tip resonant frequency due to magnetic fields emanating from the sample. Due to the lift and track process, topographic effects are removed. Except for a few tracking artifacts (dots and strips) in Fig. 4(b), the area shows a uniform contrast for the unirradiated sample, suggesting that the magnetic domains in the unirradiated film are too small to be resolved (i.e., <50 nm). This is expected because the average size of the single-domain grains is only ~3 nm, and domains larger than the detection limit (50 nm) are less probable to be present. After irradiation, the MFM image of the film is shown in Fig. 4(d). Note that the field of view for the MFM image (5 μm) is 10 times larger than that for the corresponding HIM image [Fig. 3(b)]. A clear contrast is observed in Fig. 4(d), where the brighter area represents a larger frequency shift, thus a larger magnetic gradient. From Fig. 4(d), the magnetic domain size is on the order of tens to hundreds of nanometers. The possible existence of smaller domains below the MFM spatial resolution cannot be excluded. Since the average size of the crystalline grains with single magnetic domains in the irradiated film is only 23 nm, the formation of some larger domains consisting of multiple grains occurred during the ion irradiation.

D. ac magnetic susceptibility and SIRM

The response of the magnetic properties of the unirradiated and irradiated Fe_3O_4 films to ac frequency and temperature in the zero dc field-cooling process has also been investigated in this study. The frequency dependence of the χ' data for both the

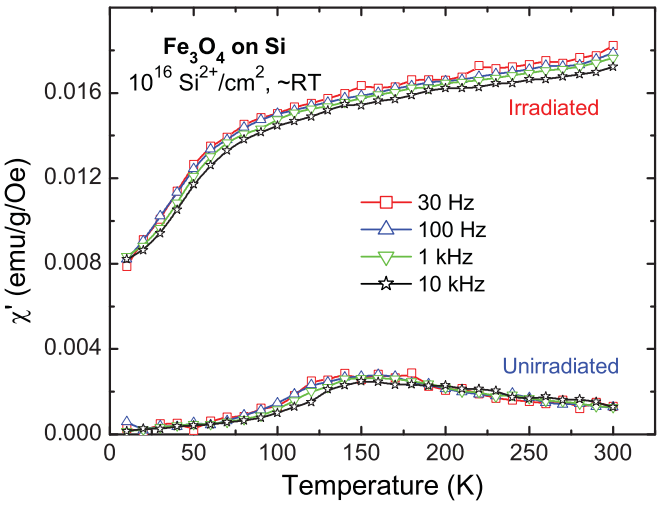

FIG. 5. (Color online) Frequency dependence of the in-phase ac magnetic susceptibility of granular Fe_3O_4 films on Si before and after irradiation.

unirradiated and irradiated films is shown in Fig. 5 as a function of temperature. In general, the χ' value for the unirradiated sample increases with decreasing temperature from 300 to 150 K and decreases at lower temperatures. Above ~150 K, the χ' value closely follows the Curie-Weiss law, demonstrating superparamagnetic behavior in the measurement time scale. Below 150 K, the χ' value decreases as the sample is further cooled, exhibiting a blocking effect. From Fig. 5, there is a shift in the blocking temperature to a higher value as frequency increases because particles of a given size show higher blocking temperatures with decreased measurement time.[24] The χ' value for the unirradiated film was fitted with peak functions. The blocking temperatures have been estimated based on the peak maxima[26] to be 147, 150, 156, and 164 K for frequencies of 0.03, 0.1, 1, and 10 kHz, respectively, as given in Table I. These values are significantly higher compared to those (~15 K) for noninteracting, horse-spleen ferritin[26] and are lower than the dc susceptibility blocking temperatures (~203 K) for undiluted, interacting oleate-capped magnetite nanocrystals (6.6 nm in size).[27] It has been shown[27,28] that the blocking temperature for both dc and ac measurements is much lower for noninteracting particles than for interacting particles in the same system. Thus, our system is expected to be interacting because of the higher blocking temperature

TABLE I. Parameters fitted to the data in Fig. 5 or the unirradiated film.

Frequency	Bl. Temp.	Curie-Weiss law	
ν_0 (kHz)	T_B (K)	T_c (K)	C (K emu/g/Oe)
0.03	147	25	0.37
0.1	150	23	0.38
1	156	25	0.38
10	164		
		Vogel-Fulcher law	
	KV/k_B (K)	τ^{-1} (Hz)	T_0 (K)
	1330	1.9×10^{12}	94

than that for a noninteracting system like ferritin,[26] but the interaction is relatively weak compared to the interacting oleate-capped magnetite particles.[27] Data fitting above the respective blocking temperatures was performed using the Curie-Weiss law,[29]

$$\chi' = C/(T - T_c), \tag{2}$$

where C and T_c are fitting parameters. The fitting results are given in Table I. The data fit at 10 kHz failed because of the high measurement noise as observed by others in a separate study.[22] From Table I, the C value is nearly the same (0.37–0.38 K emu/g/Oe) for frequencies of 0.03, 0.1, and 1 kHz, and parameter T_c has comparable values (23–25 K). Further data fitting was also carried out using the Vogel-Fulcher law,[30]

$$\tau^{-1} = f_0 \exp[-KV/k_B(T_B - T_0)], \tag{3}$$

where τ is the relaxation time, f_0 is the applied ac frequency, K is the anisotropy constant, V is the particle volume, k_B is the Boltzmann constant, and T_0 is the characteristic ordering temperature. The quantity KV represents the energy barrier of the magnetic two-level system. Excellent data fits were obtained with the results given in Table I. Compared to the ferritin study,[26] the attempt frequency τ^{-1} of 1.9×10^{12} Hz determined from this study agrees very well with the reported data. However, the KV/k_B value is significantly higher for the unirradiated Fe_3O_4 film [1330 K versus ~400 K in (Ref. 26)], indicating a higher energy barrier for activating domain reorientation. The higher energy barrier is correlated to the dipolar magnetic interactions between the nanoparticles in the film, as indicated by the nonvanishing T_0 (94 K). Since T_0 is much smaller than $T_k(= KV/k_B)$, the coupling interaction is still considered to be weak,[31] which is consistent with the assessment from the blocking temperature. Note that the attempt frequency (inverse of the relaxation time) for the unirradiated film is similar to that of canonical spin glasses,[32] but the T_0 and T_k are more similar to cluster glasses that normally have much slower relaxation times.[33] Therefore, the granular magnetite film represents a new class of semidisordered magnetite materials. It should also be noted that the attempt frequency is approximately eight orders of magnitude larger than the highest ac frequency (10^4 Hz) applied in this study. Thus, the equilibrium magnetization can be attained nearly instantly, and lagging response is insignificant. This is confirmed by the small values [10^{-5} (emu/g)/Oe] of out-of-phase susceptibility χ'' (data not shown) obtained from this study for the unirradiated film.

After irradiation, a significant increase in the χ' value is observed at the applied temperatures, from ~10^{-3} to 1.8×10^{-2} (emu/g)/Oe at 300 K and from ~10^{-4} to 8×10^{-3} (emu/g)/Oe at 10 K. For the irradiated sample, there is an observable frequency dependence in the temperature range, with a systematically lower χ' value at higher frequencies. The result can be understood because ferromagnetic materials (large Fe_3O_4 grains in this study) have strong domain interactions that can give rise to the frequency dependence. In addition, there may still remain some interacting superparamagnetic particles that have not grown to sufficient size to exhibit ferromagnetism. From Fig. 5, there are two stages in the cooling process: a nearly linear decrease in the χ' value as

temperature decreases from 300 to 75 K, followed by a more rapid decrease below 75 K.

The magnetization behavior of Fe_3O_4 at low temperatures is complex and has been studied for nearly a century. Verwey[34] proposed a theory based on electron hopping between adjacent Fe^{2+} and Fe^{3+} ions at B sites of the spinel structure in a thermally activated process. At Verwey transition temperature T_v [~125 K (Ref. 35) for bulk magnetite], thermal fluctuation cannot overcome the hopping barrier, resulting in a discontinuity in electrical conductivity and magnetic properties. However, the theory has been found to be inadequate because a later discovery[36] indicates that there is a structural transformation from cubic to triclinic phase at low temperature. Calculations[37] show that a slight structural distortion of Fe_3O_4 can significantly affect the exchange process, which is not taken into account in the Verwey theory. Although the transition is still not completely understood, considerable progress has been achieved over the past two decades.[35]

It is known that as stoichiometric Fe_3O_4 becomes progressively oxidized, the magnetic signature of the Verwey transition becomes blurred and eventually disappears as the magnetite is converted completely to maghemite (γ-Fe_2O_3).[38] However, there is no evidence from this study that indicates the formation of maghemite during ion irradiation. Maghemite has a smaller lattice constant ($a = 0.835\,15$ nm) compared to magnetite ($a = 0.8396$ nm) and its diffraction pattern should appear at a larger angle, which does not match with the diffraction pattern for the irradiated film shown in Fig. 2. Since the irradiation was performed in vacuum, and thermal annealing above room temperature was not conducted, substantial oxidation of the granular film is not expected. Therefore, we cannot ascribe the decrease in χ' entirely, if at all, to nonstoichiometry of the Fe_3O_4 particles after irradiation.

Previous experimental studies[39] of multidomain and pseudo-single-domain magnetite samples have shown that magnetite particles with different sizes, stoichiometry, and thermomagnetic treatments have a different temperature dependence of in-phase susceptibility. The results shown in Fig. 5 are different from the reported data[39] in that (i) the χ' value in this study decreases with decreasing temperature, starting from 300 K, (ii) T_v is smaller (~75 K), and (iii) the transition is more gradual. In that study,[39] the mean particle size in the four used samples was in the range from 100 nm to 100 μm, and the Verwey transition temperature and the sharpness of the transition were observed to decrease monotonically with decreasing particle size. Both the smaller T_v value and the more broadened transition at T_v observed from this study generally follow the trend for the smaller grain size. The complex structure, broad distribution of grain size, and weak interactions between particles[40] may be responsible for suppressing the Verwey transition in this study.

The nearly linear decrease in the χ' value with decreasing temperature from 300 to 75 K has not been reported in the literature for pure magnetite particles, although similar behavior of intracellular magnetite[22] and metal-deficient magnetite[40] was observed. From Fig. 5, the blocking effects already exist at room temperature and the blocking temperature is apparently above 300 K. From the discussion above, in addition to the large ferromagnetic particles (size > 30 nm) in the irradiated film, there may remain a fraction of smaller superparamagnetic

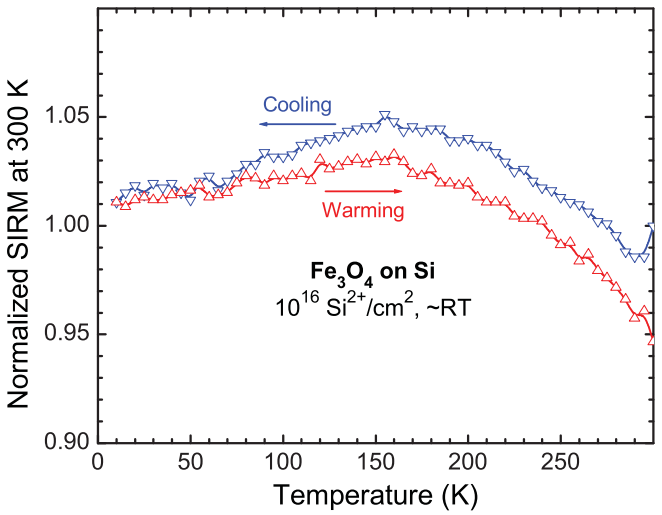

FIG. 6. (Color online) Behavior of normalized room-temperature SIRM of the irradiated film during zero-field cooling and warming cycles between 10 and 300 K.

interacting particles whose blocking temperature increases with increasing particle size. It has been reported[27] that to achieve a blocking temperature greater than 300 K, the size of interacting Fe_3O_4 particles must reach a value between 11.6 and 17.8 nm. The size distribution of the particles in the irradiated film traverses the boundaries of single stable domains and superparamagnetic regimes. This regime has been rarely reported in the literature, except for some studies of geologic samples that may contain mixed assemblages of magnetic components. Since ferromagnetic materials above T_c follow the Curie-Weiss law, i.e., magnetization increases with decreasing temperature, the data in Fig. 5 suggest that the superparamagnetic component in the irradiated film dominates the magnetic behavior even at room temperature.

Figure 6 shows the behavior of the normalized SIRM (produced at 300 K) for the irradiated film during consecutive processes of cooling from 300 to 10 K and warming from 10 to 300 K. The general behavior is similar to that observed for some intracellular magnetite particles.[22] From Fig. 6, the blocking temperature for the magnetization is ~150 K. Unlike adjacent unpaired electrons that tend to line up the magnetic moments parallel to each other because of the exchange energy of spin-spin coupling, small single domains in the irradiated granular film could reduce system energy by rotating moments to an antiparallel arrangement when cooled down with no external fields. In a single-domain particle system, it is not possible to reverse magnetization through boundary displacement; instead, the magnetization of the particle must rotate as a whole (i.e., Néel relaxation).[29,41] Again from Fig. 6, an apparent Verwey transition is not observed during either the cooling or warming cycle in this study. A recent report[42] shows a sharp Verwey transition for stoichiometric magnetite particles during zero-field warming of SIRM produced at 10 K; for the particles oxidized partially or at the surface, the transition becomes more complex and broadened, and the remanence changes across the transition are much smaller for smaller (37 nm) oxidized magnetite than for their larger (220 nm) counterparts. In the granular films of this study, the

unobservable Verwey transition is likely due to the complex structure and relatively small grain size in the irradiated film. Compared to cooling and warming curves, the temperature dependence of magnetization is essentially the same below 80 K. At higher temperatures, the magnetization behavior is similar, but the absolute value of magnetization during warming up is smaller, indicating that some domain reorientations are irreversible by thermal activation. However, the difference in the values over the temperature range is less than 6%, suggesting that most of the reorientation processes are thermally reversible. Future studies using techniques such as first-order reversal curves (FORC) are planned, which could further elucidate the relative importance of the reversible and irreversible components of magnetization.

IV. CONCLUSIONS

It has been found that the porous granular Fe_3O_4 film with an average grain size of ∼3 nm undergoes a change from superparamagnetic to ferromagnetic behavior after 5.5 MeV Si^{2+} ion irradiation to a fluence of 10^{16} ion/cm^2 near room temperature. The remnant magnetization of the film at room temperature changes from 0 to 9.4 emu/g. The magnetization at 10 kOe and coercivity for the irradiated sample increased to 56 emu/g and 250 Oe, respectively. The Fe_3O_4 average grain size is increased from ∼3 to ∼23 nm as a result of the irradiation. A dramatic change in the microstructures of the irradiated film occurs, featuring particle aggregation. Irradiated films consist of some stable domains with a fraction of superparamagnetic particles remaining. The observed magnetic domains in the irradiated film have a size of tens to hundreds of nanometers, while domains smaller than the MFM spatial resolution (50 nm) cannot be excluded. The change in the magnetic property of the granular Fe_3O_4 film is attributed to the irradiation-induced grain growth and an alteration of the interatomic and electronic configurations at the grain-particle surface and interface, which lead to magnetic domain growth, reorientation, and the occurrence of magnetic anisotropy.

There are dipolar interactions between the particles in both the unirradiated and irradiated films. The blocking temperatures for the unirradiated sample are determined to be from 147 at 30 Hz to 164 K at 10 kHz. Above ∼150 K, in-phase ac magnetic susceptibility closely follows the Curie-Weiss law. Data fit using the Vogel-Fulcher law suggest that the attempt frequency for the unirradiated film is on the order of 10^{12} Hz. The Verwey transition for the irradiated film is broad and occurs at ∼75 K, as determined from the change in slope of the ac susceptibility. The observed unusual behavior of decreasing χ' from 300 to 75 K has been attributed to the existence of superparamagnetic particles in the irradiated film with blocking temperatures above room temperature. Although most of the reorientation processes for SIRM produced at room temperature are reversible during zero-field cooling and warming cycles between 10 and 300 K, some of them are thermally irreversible, leading to a difference of less than 6% in the magnetization value.

ACKNOWLEDGMENTS

This study was supported by the Division of Materials Sciences and Engineering, Office of Basic Energy Sciences, US Department of Energy (DOE) under Contract No. DE-AC05-76RL01830 (irradiation and structural characterizations) and by the Defense Threat Research Agency, US Department of Defense, IACRO 10-4951I (magnetic property measurements). The samples were prepared at the University of Idaho, supported by DOE under Contract No. DE-FG02-07ER46386 and No. DE-FG02-04ER46142. HIM experiments were performed with assistance from Chuong Huynh at Carl Zeiss SMT. A portion of the research was performed using EMSL, a national scientific user facility sponsored by the DOE's Office of Biological and Environmental Research and located at PNNL.

*Author to whom all correspondence should be addressed: weilin.jiang@pnl.gov

[1] C. Boeglin, E. Beaurepaire, V. Halté, V. López-Flores, C. Stamm, N. Pontius, H. A. Dürr, and J.-Y. Bigot, Nature (London) **465**, 458 (2010).

[2] *Materials Science with Ion Beams, Topics in Applied Physics*, edited by H. Bernas (Springer, Berlin, 2010), vol. **116**, p. 227.

[3] *Proceedings of the 53rd Annual Conference on Magnetism and Magnetic Materials*, edited by D. H. Reich [J. Appl. Phys. **105** (2009)].

[4] P. Esquinazi, D. Spemann, R. Höhne, A. Setzer, K.-H. Han, and T. Butz, Phys. Rev. Lett. **91**, 227201 (2003).

[5] C. Chappert, H. Bernas, J. Ferré, V. Kottler, J.-P. Jamet, Y. Chen, E. Cambril, T. Devolder, F. Rousseaux, V. Mathet, and H. Launois, Science **280**, 1919 (1998).

[6] C. T. Rettner, S. Anders, J. E. E. Baglin, T. Thomson, and B. D. Terris, Appl. Phys. Lett. **80**, 279 (2002).

[7] G. J. Kusinski, K. M. Krishnan, G. Denbeaux, G. Thomas, B. D. Terris, and D. Weller, Appl. Phys. Lett. **79**, 2211 (2001).

[8] K. Zhang, K. P. Lieb, M. Marszalek, V. Milinovic, and V. Tokman, Thin Solid Films **515**, 700 (2006).

[9] M. C. Sung, D. G. You, H. S. Park, J. C. Lee, S. Y. Ie, I. S. Kim, J. Lee, C. N. Whang, S. Im, K. Jeong, T. G. Kim, J. S. Yang, and J. H. Song, J. Appl. Phys. **90**, 2036 (2001).

[10] D. Ravelosona, C. Chappert, V. Mathet, and H. Bernas, Appl. Phys. Lett. **76**, 236 (2000).

[11] S. I. Woods, S. Ingvarsson, J. R. Kirtley, H. F. Hamann, and R. H. Koch, Appl. Phys. Lett. **81**, 1267 (2002).

[12] J. A. Sundararajan, D. T. Zhang, Y. Qiang, W. Jiang, and J. S. McCloy, J. Appl. Phys. **109**, 07E324 (2011).

[13] P. Allongue and F. Maroun, MRS Bull. **35**, 761 (2010).

[14] Y. Qiang, J. Antony, A. Sharma, J. Nutting, D. Sikes, and D. Meyer, J. Nanopart. Res. **8**, 489 (2006).

[15]J. F. Ziegler, J. P. Biersack, and U. Littmark, *The Stopping and Range of Ions in Solids* (Pergamon, New York, 1985); available at [http://www.srim.org].
[16]B. D. Cullity and S. R. Stock, *Elements of X-Ray Diffraction*, 3rd ed. (Prentice Hall, Englewood Cliffs, NJ, 2001), p. 170.
[17]W. Jiang, H. Wang, I. Kim, I.-T. Bae, G. Li, P. Nachimuthu, Z. Zhu, Y. Zhang, and W. J. Weber, Phys. Rev. B **80**, 161301(R) (2009).
[18]W. Jiang, H. Wang, I. Kim, Y. Zhang, and W. J. Weber, J. Mater. Res. **25**, 2341 (2010).
[19]J. Lian, J. Zhang, F. Namavar, Y. Zhang, F. Lu, H. Haider, K. Garvin, W. J. Weber, and R. C. Ewing, Nanotechnology **20**, 245303 (2009).
[20]Y. Zhang, W. Jiang, C. M. Wang, F. Namavar, P. D. Edmondson, Z. Zhu, F. Gao, J. Lian, and W. J. Weber, Phys. Rev. B **82**, 184105 (2010).
[21]H.-U. Worm, Geophys. J. Int. **133**, 201 (1998).
[22]M. Pósfai, B. M. Moskowitz, B. Arató, D. Schüler, C. Flies, D. A. Bazylinski, and R. B. Frankel, Earth Planet. Sci. Lett. **249**, 444 (2009).
[23]D. J. Dunlop, J. Geophys. Res. **78**, 1780 (1973).
[24]J. L. Dormann, D. Fiorani, and E. Tronc, *Advances in Chemical Physics*, edited by I. Prigogine and S.A. Rice (Wiley, 1997), Vol. XCVIII, p. 283.
[25]R. Hyndman, P. Warin, J. Gierak, J. Ferré, J. N. Chapman, J. P. Jamet, V. Mathet, and C. Chappert, J. Appl. Phys. **90**, 3843 (2001).
[26]F. Luis, E. del Barco, J. M. Hernández, E. Remiro, J. Bartolomé, and J. Tejada, Phys. Rev. B **59**, 11837 (1999).
[27]D. Caruntu, G. Caruntu, and C. J. O'Connor, J. Phys. D **40**, 5801 (2007).
[28]M. F. Hansen, P. E. Jönsson, P. Nordblad, and P. Svedlindh, J. Phys. Condens. Matter **14**, 4901 (2002).
[29]C. Kittel, *Introduction to Solid State Physics*, 8th ed. (Wiley, 2005), p. 324.
[30]R. W. Chantrell and E. P. Wohlfarth, J. Magn. Magn. Mater. **40**, 1 (1983).
[31]S. Shtrikman and E. P. Wohlfarth, Phys. Lett. A **85**, 467 (1981).
[32]J. L. Tholence, Solid State Commun. **35**, 113 (1980).
[33]R. N. Bhowmik and R. Ranganathan, J. Magn. Magn. Mater. **237**, 27 (2001).
[34]E. J. W. Verwey, Nature (London) **144**, 327 (1939).
[35]F. Walz, J. Phys. Condens. Matter **14**, R285 (2002).
[36]M. Iizumi, T. F. Koetzle, G. Shirane, S. Chikazumi, M. Matsui, and S. Todo, Acta Crystallogr. Sect. B **38**, 2121 (1982).
[37]J. Garcia and G. Subia, J. Phys. Condens. Matter **16**, R145 (2004).
[38]Ö. Özdemir, D. J. Dunlop, and B. M. Moskowitz, Geophys. Res. Lett. **20**, 1671 (1993).
[39]A. Kosterov, Geophys. J. Int. **154**, 58 (2003).
[40]D. Kim, K. Hwang, C. S. Lee, J. C. Sur, H. K. Shim, and Y. I. Kim, Bull. Korean Chem. Soc. **20**, 1313 (1999).
[41]J. Zhang, C. Boyd, and W. Luo, Phys. Rev. Lett. **77**, 390 (1996).
[42]Ö. Özdemir and D. J. Dunlop, J. Geophys. Res. B **115**, 02101 (2010).